Korean J. Chem. Eng., 34(1), 249-258 (2017)
DOI: 10.1007/s11814-016-0249-5

pISSN: 0256-1115
eISSN: 1975-7220

Esterification of propionic acid with isopropyl alcohol over ion exchange resins: Optimization and kinetics

Vishal Suresh Chandane, Ajit Pralhad Rathod†, Kailas Lachchhuram Wasewar, and Shriram Shaligram Sonawane

Department of Chemical Engineering, Visvesvaraya National Institute of Technology, Nagpur-440010 (MS), India
(*Received 25 June 2016 • accepted 29 August 2016*)

Abstract−The esterification of propionic acid with isopropyl alcohol was studied in an isothermal batch reactor. The activities of three different types of ion exchange resin catalysts (Amberlyst 15, Amberlyst 70 and Dowex 50 WX8) were investigated, and Amberlyst 15 was found to be an effective catalyst for the reaction. The effects of process parameters, namely, catalyst loading, alcohol to acid molar ratio and reaction temperature, were studied and optimized. Response surface methodology (RSM) was applied to optimize the process parameters as well as to investigate the interaction between process parameters. The internal and external diffusion limitations were found to be absent at a stirring speed of 500 rpm. The RSM model predicted response (83.26%) was verified experimentally with a good agreement of experimental value (83.62±0.39%). Moreover, the kinetics was studied and the Langmuir-Hinshelwood model was used to fit the kinetic data.

Keywords: Ion Exchange Resin, Amberlyst 15, Dowex 50 WX8, Response Surface Methodology, Box-Behnken Design

INTRODUCTION

Heterogeneous catalysts have been popularly used for years in synthesis of esters by the esterification process. The most commonly used catalysts are the ion-exchange resins having sulfonic acid groups attached to polymer carriers, such as polystyrene cross-linked with divinylbenzene (DVB) [1]. The heterogeneous ion-exchange resins have gained more attention in recent years due to several advantages over homogeneous catalyst, including removal from reaction mixture, elimination of side reactions, high product purity, good thermal stability and non-corrosive nature [2,3].

Typically, esterification reactions are very slow, chemical equilibrium limited and require several days to reach the equilibrium in absence of a catalyst [4]. Catalysts are required to accelerate the esterification reaction. For this purpose, both homogeneous and heterogeneous catalysts can be used. Few homogeneous catalysts such as sulfuric acid and *p*-toluene sulfonic acid have strong catalytic effect but suffer with several limitations like equipment corrosion, side reactions and product purification [5]. However, in most of the recent studies heterogeneous catalysts have been used successfully avoiding limitations of homogeneous catalysts [6-9].

Among wide variety of ion exchange resins, the cation exchange resins are most commonly used as heterogeneous catalyst in esterification reaction. The ion exchange resins not only catalyze the esterification reaction but also influence the equilibrium conversion of the esterification due to their selective adsorption capacity and swellability [10].

The effects of various ion exchange resins were studied in esterification reactions in previous reports, such as esterification of acetic acid with isoamyl alcohol in presence of Purolite CT-175 [11], propionic acid esterification with methanol, ethanol and 1-butanol using Amberlyst-15 [3], liquid phase esterification of mixed succinic/acetic acid with ethanol using Amberlyst-70 [12], esterification of glutaric acid with methanol using Amberlyst-35 [13], esterification of acetic acid ethylene glycol using Amberlyst-36 [14] and esterification of acrylic acid with propylene glycol in presence of Amberlyst-36 [15]. In addition, an esterification reaction using other ion exchange resins such as Dowex resin [16,17], Amberlite IR-120 [18-20], Indion 130 and Indion 190 [10] was also reported.

Isopropyl propionate is a colorless liquid with an odor reminiscent of banana and pineapple. It is used as a solvent and flavor modifier in various chemical industries. To the best our knowledge there are no reports on esterification of propionic acid with isopropyl alcohol in presence of ion exchange resins so far.

Response surface methodology (RSM) is an efficient statistical technique used to optimize operating process parameters, building models and estimation of various factors on desirable response. It significantly allows the user to collect large information from less number of experiments and also it provides the possibility of observing the effects of individual variable and their combinations of interactions on the response [21].

In the present work, esterification of propionic acid and isopropyl alcohol in presence of Amberlyst-70, Amberlyst-15 and Dowex 50 WX8 was investigated and their activities were determined. The esterification reaction was performed in an isothermal batch reactor using the catalyst with the highest activity. The effects of various operating process parameters such as catalyst loading, molar ratio of alcohol to acid, reaction temperature, stirring speed and particle size of catalyst on the conversion of propionic acid were investigated. RSM was employed to optimize the operating param-

†To whom correspondence should be addressed.
E-mail: ajitprathod@gmail.com

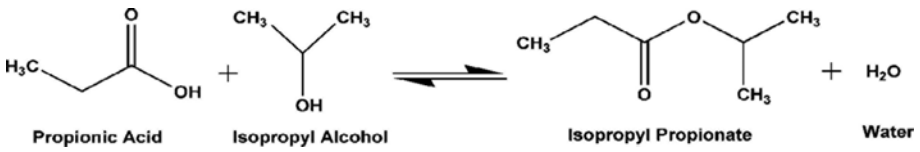

Scheme 1. Esterification of propionic acid and isopropyl alcohol.

Table 1. Physico-chemical properties of cation exchange resins used in the study

	Amberlyst 15	Amberlyst 70	Dowex 50 WX8
Manufacturer	Dow Chemical Co.	Rohm & Haas	Rohm & Haas
Physical form	Gray colored spherical beads	Dark brown colored spherical beads	Light brown colored grains
Matrix type	Styrene-DVB	Styrene-DVB	Styrene-DVB
Polymer type	Macro reticular	Micro porous	Gel (micro porous)
Ionic form	H^+	H^+	H^+
Functional group	Sulfonic acid	Sulfonic acid	Sulfonic acid
Ion exchange capacity (eq L^{-1})	1.8	0.9	1.7
Particle size (mm)	0.600-0.800	0.04-0.07	0.50
Thermal stability (°C)	120	190	150
Moisture holding capacity (%)	52-57	53-59	50-58

eters namely catalyst loading, molar ratio of alcohol to acid and reaction temperature. Moreover, the Langmuir-Hinshelwood model was used to describe the kinetics of reaction and kinetic parameters were evaluated. The general reaction scheme for esterification of propionic acid and isopropyl alcohol is given in Scheme 1.

EXPERIMENTAL

1. Chemicals

All chemicals were of analytical grade. Propionic acid (purity >99%) and isopropyl alcohol (purity >99%) were procured from Merck and used without further purification. Methanol and Karl Fischer reagent were purchased from Rankem Chem. Ltd. (Mumbai, India). Cation exchange resins, Amberlyst 15 and Amberlyst 70 were purchased from S.D. fine chem. Ltd. (Mumbai, India) and Dowex 50 WX8 was procured from Sigma-Aldrich. Catalysts were dried at 363 K to remove moisture present if any. The physico-chemical properties of cation exchange resins used in the study are listed in Table 1.

2. Experimental Procedure

2-1. Determination of Ion Exchange Capacity of Resins

The ion exchange capacity of each resin was confirmed experimentally. In a typical test, 1 g of dried resin was dispersed in 50 mL of 1 M NaCl solution and ultrasonicated for 1 hr. Then, resin was filtered and the filtrate was titrated against 0.1 N NaOH using phenolphthalein as an indicator. The acid site concentration (average of three measurements) obtained by difference was 1.72±0.05 eq L^{-1} for Amberlyst 15, 0.83±0.03 eq L^{-1} for Amberlyst 70, 1.65± 0.05 eq L^{-1} for Dowex 50 WX8, in agreement with the values reported by manufacturer.

2-2. Esterification Reaction

The esterification reaction was performed in a 250 mL three neck round-bottom flask which was heated on a rotamantle. The flask was equipped with a reflux condenser to prevent loss of the volatile components. The reaction system was stirred with magnetic stirrer, and temperature inside the flask was controlled by PID temperature controller. Initially, isopropyl alcohol was taken in a three-neck flask and heated to the required temperature. Once the temperature was reached, the propionic acid at the same temperature was added to the three neck flask followed by addition of catalyst. This time was considered as zero time. Aliquots of samples were withdrawn at every 15 min during first two hours and every 30 min during next hours. The samples withdrawn were immediately transferred to cold water to cease the reaction completely.

2-3. Analysis

Experiments were repeated three times to ensure the reproducibility of the results. The concentration of propionic acid in the reaction mixture was evaluated by titration method using 0.1 N NaOH with phenolphthalein as an indicator. The NaOH was standardized with 0.1 N oxalic acid. The water formed during the reaction was measured by Microprocessor based Karl Fischer titrator (Optics Technology, India). After verifying that the measured water content corresponds to the calculated values based on stoichiometric equation, it was concluded that there was no by product formation.

3. Experimental Design and Optimization by RSM

The independent variables chosen were included catalyst loading (X_1), molar ratio of alcohol to acid (X_2) and reaction temperature (X_3). The propionic acid conversion was chosen to be the response variable (Y) of the experimental design. For each selected variable, the experimental range and central point (in terms of actual and coded levels) are tabulated in Table 2. Seventeen sets of individual experiments were conducted according to the standard Box-Behnken experimental design (BBD) with three process variables at three levels. Design Expert Version 9.0.6 (US, State-Ease Inc.) software was used for design of experiments and to analyze the experimental data.

Table 2. Selected independent factors in coded form used in Box-Behnken design

Variables	Symbol	Coded levels		
		−1	0	+1
Catalyst loading (% w/w)	X_1	7	9	11
Molar ratio of alcohol to acid (M)	X_2	1	2	3
Reaction temperature (K)	X_3	333	343	353

The second-order model equation was applied to predict the optimum value and to elucidate the interaction between the individual variable and response of the experimental design. The quadratic model equation recommended by RSM was expressed as Eq. (1):

$$Y = \lambda_0 + \sum_{i=1}^{k} \lambda_i X_i + \sum_{i=1}^{k} \lambda_{ii} X_i^2 + \sum_{i=1}^{k} \lambda_{ij} X_i X_{ij} + e \quad (1)$$

where, λ_0, λ_i, λ_{ii}, and λ_{ij} are the regression coefficients (λ_0 is the constant term, λ_i is the linear term, λ_{ii} is the squared term for variable i, and λ_{ij} is the interaction term between variable i and j) and Y is the predicted response variable. The k is the total number of variables used to optimize the propionic acid conversion and e is a random error.

RESULTS AND DISCUSSION

1. Effect of Catalyst Type

In the experiments, three different types of ion exchange resins, Amberlyst 15, Amberlyst 70 and Dowex 50 WX8, were tested. Experiments were performed at 353 K with molar ratio of alcohol to acid (M) 2 : 1 and catalyst loading 5% (w/w) and the results are presented in Fig. 1. It was observed that Amberlyst 15 accelerated the reaction rate more and gave the highest conversion followed by Dowex 50 WX8, while lowest conversion was observed for Amberlyst 70. The observed trend can be ascribed to the difference in H^+ ion concentration on the surface of catalyst and their pore size distribution [22]. Thus Amberlyst 15 was chosen as ion exchange catalyst for further studies.

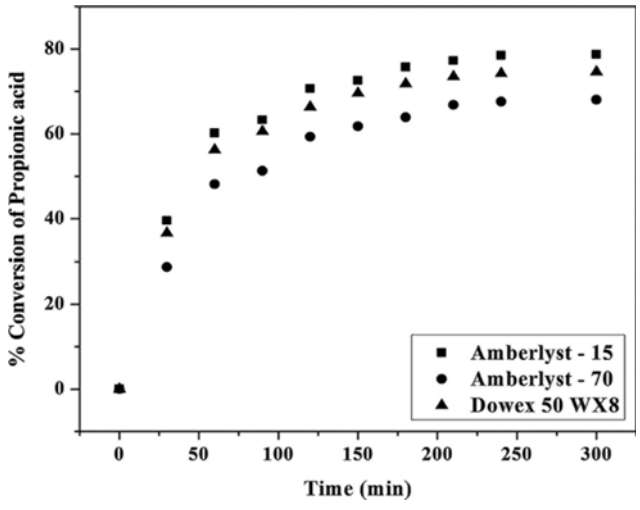

Fig. 1. Effect of catalyst type on propionic acid conversion at M=2, T=353 K, Catalyst loading 5% (w/w).

2. Influence of External Mass Transfer

Experiments were performed at the operating conditions mentioned in Section 3.1 by varying the stirring speeds from 300-800 rpm to investigate the effect of external heat and mass transfer. The conversion was low at 300 rpm, which increased further at 500 rpm. After 500 rpm no significant increase was observed up to 800 rpm. These results showed that there was negligible effect of stirring speed on the rate of reaction as followed by conversion of propionic acid above 500 rpm. This indicates the absence of external mass transfer resistance and hence, all the experiments were performed at a stirring speed of 500 rpm [23].

3. Influence of Internal Mass Transfer

The effect of internal mass transfer resistance was investigated by estimating observable modulus ($\eta\phi^2$) and employing Weisz-Prater criterion as Eq. (2), [24].

$$\phi = \frac{r^2 k}{9 D_e} \quad (2)$$

where, r and k are the radius of catalyst particle and rate constant for reaction respectively. D_e is the effective diffusion coefficient and ϕ is the Thiele modulus. Further, D_e can be evaluated as Eq. (3),

$$D_e = \frac{\varepsilon D_A}{\zeta} \quad (3)$$

where, ε and ζ are the porosity and tortuosity of catalyst particle respectively. Generally, for resin catalysts ε/ζ values are between 0.12 and 0.50. For Amberlyst 15, it was taken as 0.12 [25]. D_A is liquid phase diffusion coefficient obtained from Wilke-Chang equation [24]. By assuming initial rate to be maximum, the effectiveness factor (η) was evaluated from observable modulus as [12];

$$\eta = \frac{\tanh\phi}{\phi} \quad (4)$$

Values of D_e, D_A, ϕ and η are presented in Table 3. The value of ϕ is less than 1 and the value of effectiveness factor obtained as 0.999. This explains the absence of internal mass transfer resistance.

This outcome was further confirmed by performing experiments under similar operating conditions using the catalyst in its original form and by converting it into powdered form. Results are presented in Fig. 2, which indicate that original and powdered catalyst exhibited same effectiveness and no pore diffusion limitation was detected [26]. Hence the influence of internal diffusion was neglected.

Table 3. Estimation of internal mass transfer resistance at different temperatures using Weisz-Prater criterion

Temperature (K)	$D_A \times 10^{-9}$ ($m^2\ s^{-1}$)	$D_e \times 10^{-10}$ ($m^2\ s^{-1}$)	$\phi \times 10^{-4}$	η
323	3.5719	4.2863	5.474	0.999
333	3.6760	4.4113	5.319	0.999
343	3.7802	4.5362	5.173	0.999
353	3.8843	4.6612	5.034	0.999

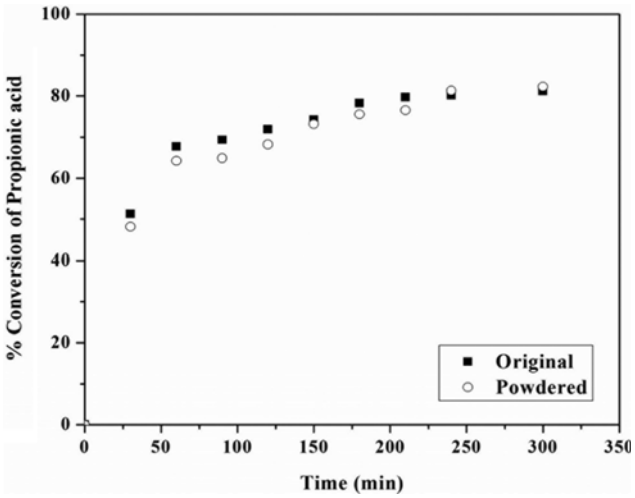

Fig. 2. Conversion of esterification of propionic acid for original and powdered catalyst.

4. Effect of Catalyst Loading

There is significant role of catalyst in increasing the overall conversion by enhancing the rate of reaction. In this study catalyst loading was varied between 1% (w/w) to 11% (w/w) at a temperature 353 K, molar ratio of alcohol to acid 2 : 1 and stirrer speed of 500 rpm. The conversion of propionic acid with respect to time at different catalyst loading is presented in Fig. 3(a), which depicts that higher the catalyst loading, faster is the rate of reaction. This is due to the higher number of total active sites available for ion exchange, which enhanced the conversion. Also, the conversion of propionic acid increased significantly from catalyst loading 1% (w/w) to 9% (w/w). However, if catalyst loading was increased after 9-11% (w/w), the conversion of propionic acid did not show significant increase [2].

This result was further confirmed by calculating the initial rate of reaction for different catalyst loading. The initial reaction rate was calculated as,

$$-r_{A0} = \frac{C_{A0} X_A}{t} \quad (4)$$

where, r_{A0} is the initial reaction rate, C_{A0} is the initial concentration of propionic acid and X_A is the conversion of propionic acid at time t. A plot of initial reaction rate vs. catalyst loading is given in Fig. 3(b), which shows that the initial reaction rate increased linearly with catalyst loading. The intercept of this plot gave the reaction rate for uncatalyzed reaction at the given conditions [10]. The mathematical relation between initial reaction rate and catalyst loading was obtained from Fig. 3(b) as,

$$-r_{A0}\ (\text{mol L}^{-1}\text{min}^{-1}) = 0.544\ X\ (\text{gm L}^{-1}) + 0.027 \quad (5)$$

where, X is catalyst loading. The expression is valid only at temperature of 353 K and molar ratio of alcohol to acid 2 : 1 at which this study was performed.

5. Effect of Molar Ratio

The esterification of propionic acid and isopropyl alcohol is limited by chemical equilibrium, and the point of equilibrium controls the amount of ester formed. The excess use of alcohol shifts the equilibrium towards the forward direction increasing the conversion of propionic acid [2]. In this study, the molar ratio of alcohol to acid was varied from 1 : 1 to 3 : 1 at a temperature 353 K, catalyst loading 9% (w/w) and stirrer speed of 500 rpm. The results are shown in Fig. 4(a), which shows that the conversion of propionic acid increased with increase in the molar ratio. However, the conversion of propionic acid from molar ratio 2 : 1 to 3 : 1 was not much significant.

6. Effect of Temperature

The esterification reaction was in the temperature range of 323-353 K at molar ratio of alcohol to acid 2 : 1, catalyst loading 9% (w/w) and stirrer speed of 500 rpm. The effect of temperature on conversion of propionic acid is shown in Fig. 4(b), which indicates that the conversion of propionic acid increased with increase in the temperature. Thus, the higher temperature is apparently favoring the acceleration of reaction to forward direction. In addition, time for the conversion to reach steady state reduced as the temperature was increased.

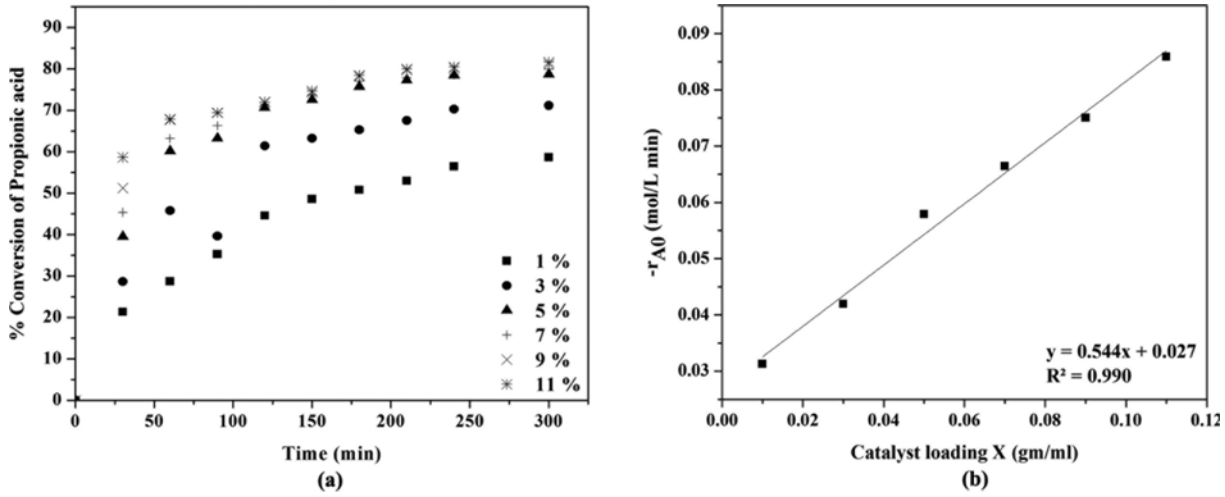

Fig. 3. Effect of different catalyst loading on propionic acid conversion.

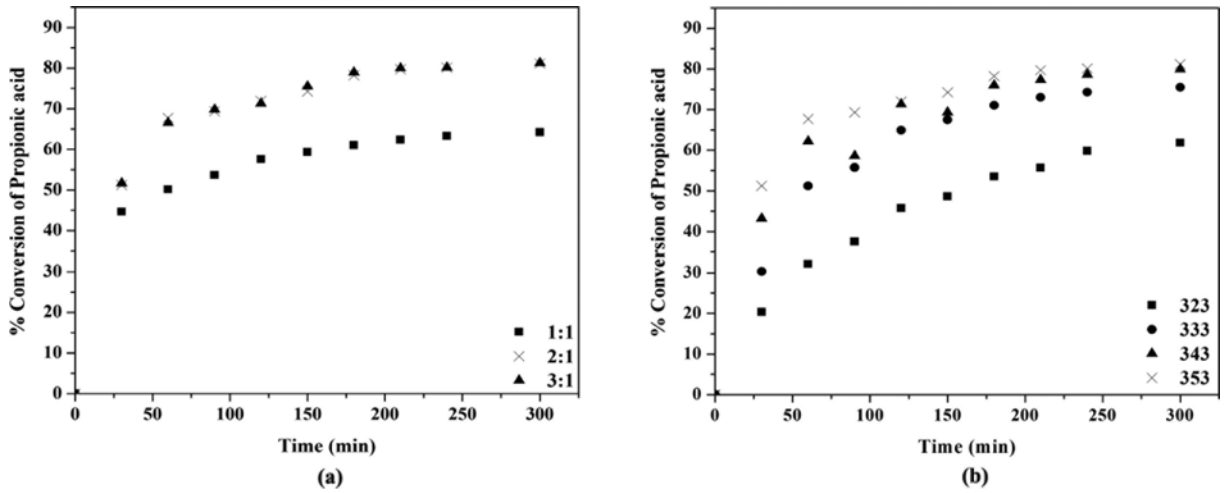

Fig. 4. Effect of alcohol to acid molar ratio and temperature on propionic acid conversion.

7. RSM Analysis

7-1. Model Determination

Table 4 gives the statistical summary of each model that was suggested by Design Expert software. The linear and 2FI model had very low R^2 and Adj.R^2 value and thus they were not adequate for experimental data. The cubic model had high R^2 and Adj.R^2 value, but it was aliased (Table 4), which means that the effects of each individual variable that cause different signals become indistinguishable. The quadratic model was suggested by the software and therefore was chosen to fit the experimental data.

Table 4. Statistical summary for each model

Model	p-value	R^2	Adjusted R^2	Suggestion
Linear	0.0021	0.6641	0.5865	Not adequate
2 FI	0.7797	0.5156	0.1103	Not adequate
Quadratic	<0.0001	0.9864	0.9689	Suggested
Cubic	-	1.00	1.00	Aliased

Table 5. Experimental data and predicted values for three process variables at three levels

Run	Experimental variables			Conversion (%)	
	X_1	X_2	X_3	Experimental	Predicted
1	11	2	353	81.62	81.63
2	7	1	343	60.59	61.43
3	9	2	343	80.92	80.92
4	9	2	343	80.92	80.92
5	9	2	343	80.92	80.92
6	9	2	343	80.92	80.92
7	9	1	353	64.18	67.46
8	7	2	333	70.05	70.04
9	9	3	353	82.25	83.08
10	11	3	343	82.92	81.08
11	11	2	333	77.34	78.86
12	9	3	333	76.18	75.50
13	11	1	343	72.46	71.77
14	9	1	333	67.05	66.22
15	9	2	343	80.92	80.92
16	7	2	353	77.59	76.07
17	0	3	343	76.34	77.03

7-2. Model Fitting and Analysis of Variance (ANOVA)

A Box-Behnken center united design was employed to design the experiments and the results obtained after performing seventeen sets of experiments for the fixed reaction time of 6 hr are tabulated in Table 5.

The best-fitting models were generated by multiregression and backward elimination. Each value reported in Table 5 was obtained as an average of three measurements. Table 5 also represents the predicted value of propionic acid conversion.

The relationship between selected independent process variables and response variable generated by RSM model is expressed as:

$$Y=+80.92+3.60X_1+6.23X_2+2.20X_3-2.25X_1^2-5.84X_2^2-2.02X_3^2 - 1.57X_1X_2-0.82X_1X_3+1.58X_2X_3 \quad (6)$$

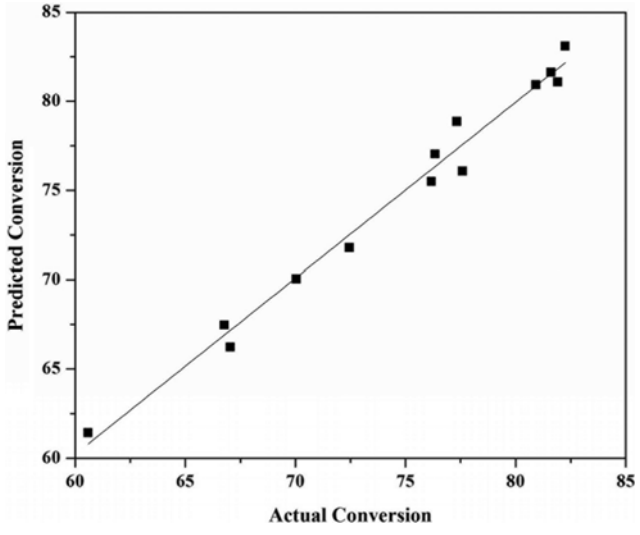

Fig. 5. Predicted vs. actual conversion of propionic acid.

where, Y is the propionic acid conversion. The linear coefficient of molar ratio is largest among all other linear coefficients, and thus the molar ratio (X_2) has the strongest effect on response variable. The next significant term is catalyst loading (X_1), followed by reaction temperature (X_3). Fig. 5 illustrates a good linear correlation between predicted and actual conversion of propionic acid (evaluated from Eq. (6)), which indicates that the model is highly significant.

ANOVA test results give the statistical significance of each variable within the experimental range and are tabulated in Table 6. The Model F-value of 56.36 implies the model is significant and there is only a 0.01% chance that an F-value this large could occur due to noise. The values $p<0.05$ indicate significant model terms. In the present case, X_1, X_2, X_3, X_1X_2, X_1X_3, X_1^2, X_2^2 and X_3^2 are significant model terms. The coefficient of determination (R^2) of 0.9864 indicated that the model could explain 98.64% of the variability. The R^2 predicted of 0.7822 is in reasonable agreement with the adjusted R^2 of 0.9689 as their difference is less than 2. Adequate precision measures the signal-to-noise ratio. A ratio greater than 4 is desirable. In the present case, an adequate precision value of 24.521 indicates an adequate signal, and this model can be applied to navigate the design space.

7-3. Effect of Process Variables on Propionic Acid Conversion

The relationships of process parameters on the response variable were evaluated by response surface plots, and Eq. (6) was used to generate those response surface plots. The three-dimensional (3D) surface plots and two-dimensional (2D) contour plots displayed in Figs. 6 to 8 indicate the propionic acid conversion as a function of two parameters by keeping the other parameter at its zero level. The circular contour plot depicts negligible interaction, whereas elliptical contour plot depicts the significant interaction between

Table 6. ANOVA results for acquired model

Source	Sum of squares	Degrees of freedom	Mean square	F-value	p-value	Characteristics
Model	671.99	9	74.67	56.36	<0.0001	Significant
X_1	103.46	1	103.46	78.10	<0.0001	
X_2	310.13	1	310.13	234.09	<0.0001	
X_3	38.81	1	38.81	29.29	0.0010	
X_1X_2	9.89	1	9.89	7.47	0.0292	
X_1X_3	2.66	1	2.66	2.01	0.1997	
X_2X_3	10.05	1	10.05	7.59	0.0283	
X_1^2	21.39	1	21.39	16.14	0.0051	
X_2^2	143.54	1	143.54	108.35	<0.0001	
X_3^2	17.12	1	17.12	12.92	0.0088	
Residual	9.27	7	1.32			
Lack of Fit	9.27	3	3.09			
Pure Error	0.000	4	0.000			
Cor Total	681.26	16				

R^2=0.9864; Adjusted R^2=0.9689

Predicted R^2=0.7822; Adequate precision=24.521

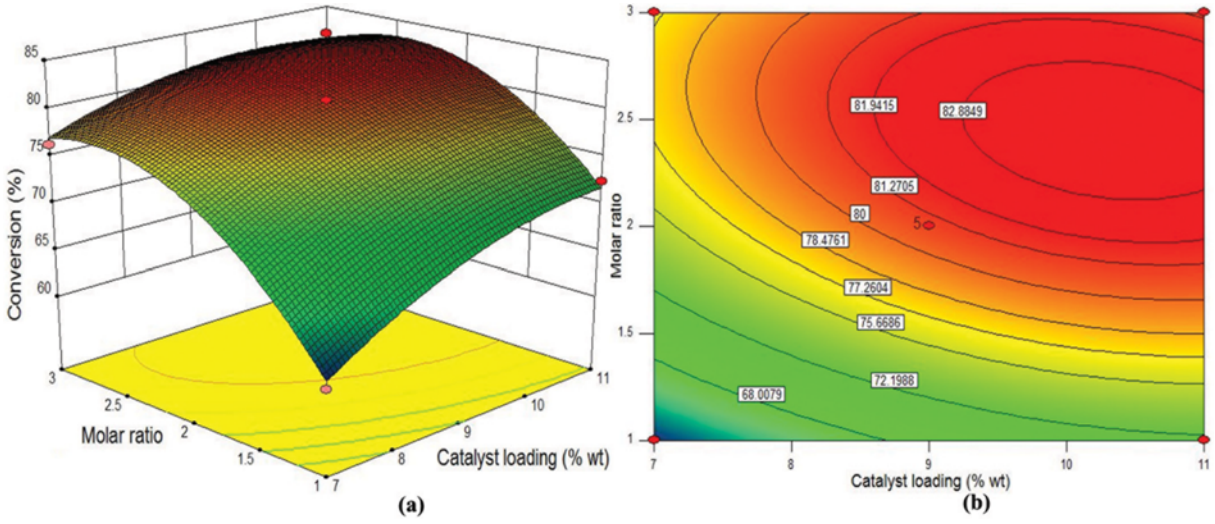

Fig. 6. Effect of molar ratio and catalyst loading on propionic acid conversion keeping temperature at its zero level: (a) Response surface plot; (b) contour plot.

corresponding variables [27]. Fig. 6(a) and (b) depicts the interaction of molar ratio and catalyst loading on propionic acid conversion. As can be seen, enhancing the amount of molar ratio as well as catalyst loading could bring about high conversion of propionic acid. More catalyst reveals more active sites which take part in the reaction and increase the conversion. The elliptical contour plot indicated that the combined effect of molar ratio and catalyst loading was significant. This result is also supported by lower p-value (0.0292) of interaction effect X_1X_2 term (Table 6).

Fig. 7(a) and (b) represents the effect of temperature and catalyst loading on propionic acid conversion. It is evident that the propionic acid conversion slightly increased by increasing the reaction temperature. At low catalyst loading, the conversion increased with slightly increasing temperature. However, at higher catalyst loading, the propionic acid conversion increased moderately with increase in reaction temperature. Thus, the reaction temperature plays a crucial role in determining the rate of esterification reaction [28]. The circular contour plot illustrates that the combined effect of temperature and catalyst loading is insignificant. This result is also supported by p-value >0.05 (0.1997) of interaction effect X_1X_3 term (Table 6).

The interaction effect of temperature and molar ratio on propionic acid conversion is depicted in Fig. 8(a) and (b). As can be seen, the propionic acid conversion increased with increase in molar ratio at same reaction temperature. However, after a certain molar ratio, decrease in the conversion of acid was observed, which may be due to slight deactivation catalyst. The interaction effect of the two variables was significant with elliptical shape of contour curve and with low p-value (0.0283) of the interaction term X_2X_3 (Table 6).

7-4. Optimization of Process Parameters

The optimal condition for the esterification reaction is obtained

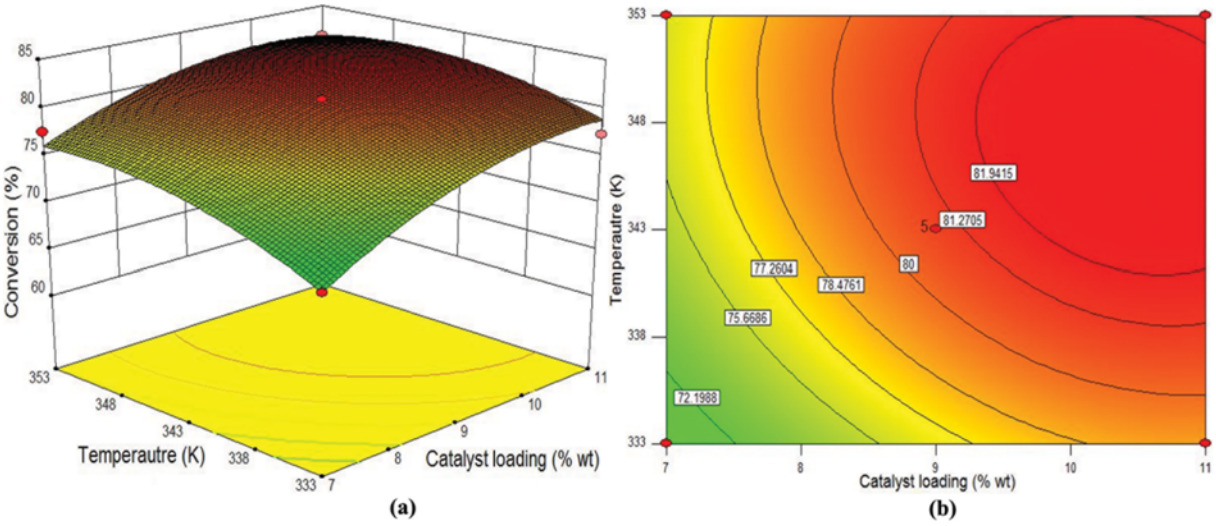

Fig. 7. Effect of temperature and catalyst loading on propionic acid conversion keeping Molar Ratio at its zero level: (a) Response surface plot; (b) contour plot.

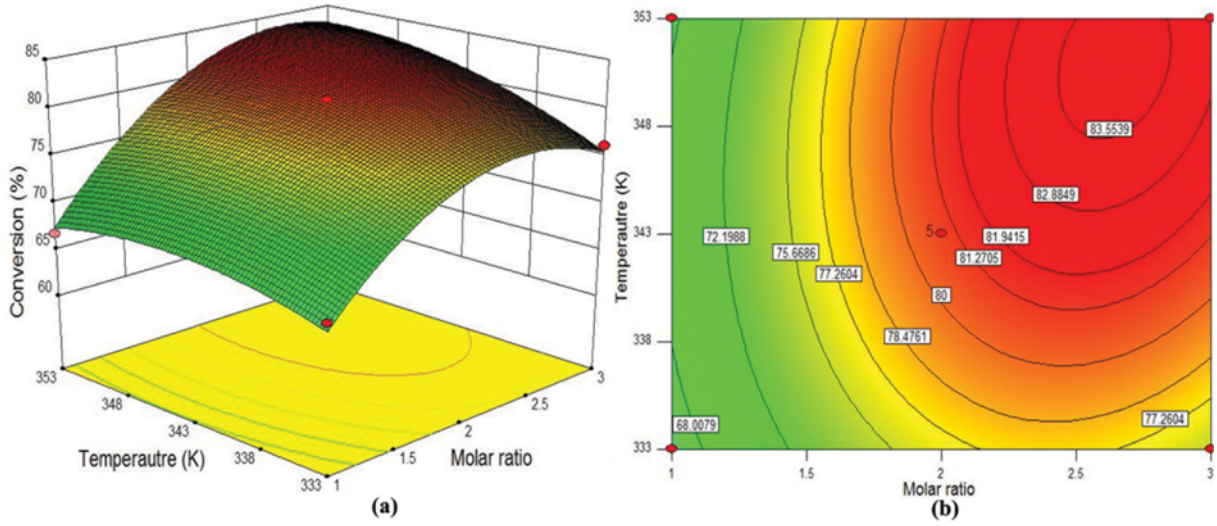

Fig. 8. Effect of temperature and molar ratio on propionic acid conversion keeping catalyst loading at its zero level: (a) Response surface plot; (b) contour plot.

Table 7. Model validation and optimal condition for the esterification reaction

Parameters	Catalyst loading, X_1 (% w/w)	Molar ratio (alcohol to acid), X_2	Temperature, X_3 (K)	Conversion of propionic acid (%)
Predicted	9.178	2.444	345	83.260
Experimental	9.2	2.5	345	83.62±0.39

by numerical optimization feature of the software Design Expert Version 9.0.6. In a typical feature, the three independent variables were set within the range from low (−1) to high (+1), whereas the response variable was set to maximize the value within minimum and maximum conversion. About 100 solutions were generated by the software, and the solution with highest desirability and maximum conversion was chosen to be verified by experiments. The optimal conditions, predicted value and the experimental value (average of three experimental measurements) of conversion, are in Table 7.

8. Kinetic Modeling

In heterogeneous catalytic reactions, the active force at the surface of catalyst distorts or dissociates the adsorbed reactant molecule to enhance the rate of reaction. The reactions using ion exchange catalyst can be categorized as quasi-homogeneous or quasi-heterogeneous reactions [10], and the kinetic orders are same in both cases. The reaction was performed under optimized conditions at different reaction temperature (333-353 K). The maximum variation in conversion of propionic acid in the temperature range 333-353 K and the same was employed for kinetic study. The kinetics can be expressed using Langmuir-Hinshelwood model by assuming that surface reaction is rate controlling and adsorption is weak for all components. For ion exchange resins, the rate equation based on Langmuir-Hinshelwood model is expressed as follows [29]:

$$\frac{dC_A}{dt} = k_f(C_A C_B - C_E C_W/K) \tag{7}$$

where, k_f is forward rate constant, K is equilibrium constant and C_A, C_B, C_C, C_D are the concentrations (mol L^{-1}) of acid, alcohol, ester and water, respectively. Eq. (7) is the power law model generally used for homogeneous reactions. In the absence of both the external and internal mass transfer resistances, the kinetics can be evaluated from the experimental data. The equilibrium constant K (k_f/k_b) can be calculated experimentally as Eq. (8),

$$K = \frac{X_e^2}{(1-X_e)(M-X_e)} \tag{8}$$

where, X_e is the equilibrium conversion of propionic acid, k_b is the backward rate constant and $M=C_{BO}/C_{AO}$ where C_{BO} and C_{AO} are the initial concentrations of alcohol and acid, respectively. In this study, equilibrium constants were calculated at three different temperatures under optimized conditions. The forward rate constant

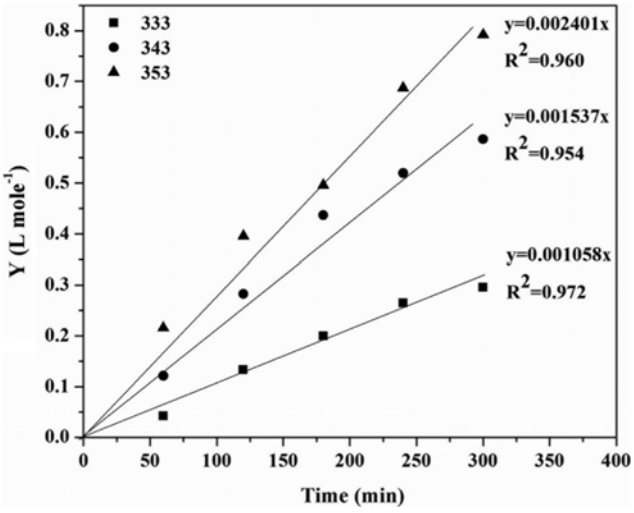

Fig. 9. Y vs. t of Eq. (9).

k_f was determined solving Eq. (7), which is as follows:

$$\frac{1}{\sqrt{B^2-4AC}}\ln\left[\frac{(B+\sqrt{B^2-4AC})C_C+2C}{(B-\sqrt{B^2-4AC})C_C+2C}\right] = Y = k_f t \tag{9}$$

where, A=(1−1/K), B=−a−b−d/K, C=ab, where a, b, d are the initial concentrations of isopropyl alcohol, propionic acid and water, respectively. The left hand side of Eq. (9) is equated to single variable Y (L mol^{-1}). The relationship between Y vs. t at different temperatures is presented in Fig. 9.

From Fig. 9, it is observed that Y relates linearly with t through origin irrespective of temperatures of reaction. This linear relationship reveals the esterification of propionic acid and isopropyl alcohol catalyzed by Amberlyst 15 is quasi-homogeneous, and Eq. (9) is used to explain the kinetics of reaction [10]. The forward rate constant k_f is evaluated from slope of this plot and subsequently backward rate constant k_b is evaluated from K and k_f. The values of K, k_f, k_b are tabulated in Table 8.

9. Activation Energy, Enthalpy and Entropy, Free Energy

The temperature dependence of reaction is expressed by Arrhenius equation as follows:

$$\ln k_f = \ln k_i^0 - \frac{E_i}{RT} \tag{10}$$

Table 8. Rate constants and free energy at different temperatures

Temperature (K)	K	k_f (L mol^{-1} min^{-1})	k_b (L mol^{-1} min^{-1})	ΔG^o (kJ mol^{-1})
333	2.0134	0.00106	0.000525	−1.94
343	2.4402	0.00184	0.000753	−2.54
353	3.2081	0.00299	0.000932	−3.42

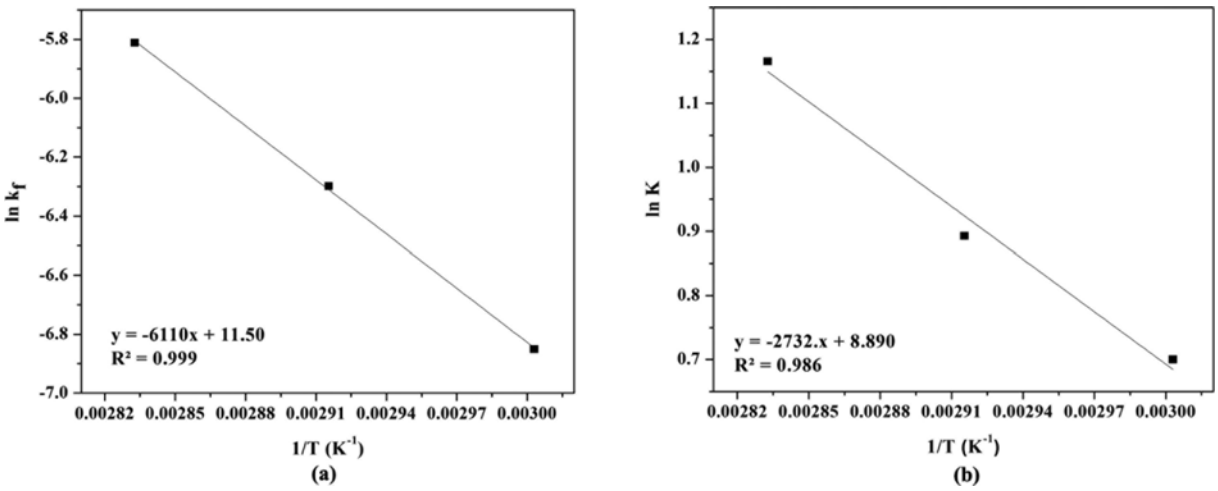

Fig. 10. Plots for finding the activation energy, pre-exponential factor and heat of reaction.

where, E_i is the activation energy and k_i^0 is the pre-exponential factor. The value of k_f is used in the evaluation of activation energy of the reaction. A plot between ln k_f and 1/T based on Eq. (10) is presented in Fig. 10(a).

The straight line of the plot revealed that the internal diffusion is not significant [19]. The activation energy is obtained from slope and pre-exponential factor were obtained by linear regression using the software Origin Pro 8. The activation energy and pre-exponential factor for the reaction were obtained to be 50.80 kJ mol^{-1} and 98,715.77 L mol^{-1} min^{-1}, respectively.

The relationship between temperature dependency and equilibrium constant is expressed by the van't Hoff equation as follows [30]:

$$\ln K = \left(\frac{-\Delta H^o}{RT}\right) + \left(\frac{\Delta S^o}{R}\right) \quad (11)$$

where, ΔH^o is the enthalpy and ΔS^o is the entropy of the reaction. Fig. 10(b) shows the relationship between ln K vs. 1/T. The negative slope reveals the endothermic nature of the reaction. The enthalpy was calculated from slope of the line, and intercept gives entropy of the reaction. The reaction enthalpy and entropy were obtained as 22.71 kJ mol^{-1} and 73.91 kJ mol^{-1} K^{-1}), respectively. The higher temperature favored the reaction, which in turn increased the equilibrium constant and hence increased the conversion of propionic acid. This was further verified by comparing the forward activation energy (50.80 kJ mol^{-1}), which was found to be greater than the backward activation energy (28.07 kJ mol^{-1}).

The free energy of the reaction was evaluated by using the following equation:

$$\Delta G^o = -RT \ln K \quad (12)$$

The ΔG^o values evaluated at different temperatures are presented in Table 8.

CONCLUSIONS

The activities of three different types of cation exchange resin catalysts (Amberlyst 15, Amberlyst 70 and Dowex 50 WX8) were studied for the esterification of propionic acid with isopropyl alcohol in an isothermal batch reactor. The order of catalytic activity of resin catalysts was obtained to be Amberlyst 15>Dowex 50 WX8 >Amberlyst 70. Experiments were carried out at a stirring speed of 500 rpm to eliminate of external diffusion limitations. The internal diffusion limitation was found to be absent as evaluated by Weisz-Prater criterion and also verified experimentally. The optimum conditions for maximum propionic acid conversion were obtained by RSM with Box-Behnken center united design with minimum experimental work. At optimal conditions (catalyst loading of 9.178% (w/w), molar ratio of 2.444 and reaction temperature of 345 K), the propionic acid conversion was 83.26%. Validation was also carried out to verify the accuracy of model, and the predicted value was found to be in good agreement with experimental value (83.71±0.37%). The Langmuir-Hinshelwood model was developed to predict the kinetic data. The activation energy and pre-exponential factor was evaluated by employing Arrhenius equation and obtained as 50.80 kJ mol^{-1} and 98,715.77 L mol^{-1} min^{-1}, respectively. The reaction enthalpy and entropy was evaluated by van't Hoff equation and found that reaction is endothermic.

TABLE OF NOMENCLATURE

X_1	: catalyst loading % [w/w]
X_2	: molar ratio of alcohol to acid
X_3	: reaction temperature [K]
Y	: response variable
λ	: regression coefficient
k	: total number of variables
e	: random error
r	: radius of catalyst particle [μm]
k	: rate constant for reaction
D_e	: effective diffusion coefficient [m^2s^{-1}]
ϕ	: thiele modulus
ε	: porosity of catalyst particle
ζ	: tortuosity of catalyst particle
D_a	: liquid phase diffusion coefficient [m^2s^{-1}]
η	: effectiveness factor

r_{A0} : initial reaction rate [mol L^{-1} min^{-1}]
C_{A0} : initial concentration of propionic acid [mol L^{-1}]
X_A : conversion of propionic acid
X_e : equilibrium conversion of propionic acid
t : reaction time [hr]
k_f : forward rate constant [L mol^{-1} min^{-1}]
k_b : backward rate constant [L mol^{-1} min^{-1}]
K : equilibrium constant
C_A : concentrations of propionic acid [mol L^{-1}]
C_B : concentrations of alcohol [mol L^{-1}]
C_C : concentrations of ester [mol L^{-1}]
C_D : concentrations of water [mol L^{-1}]
C_{AO} : initial concentrations of acid [mol L^{-1}]
C_{BO} : initial concentrations of alcohol [mol L^{-1}]
E_i : activation energy [kJ mol^{-1}]
k_i^0 : pre-exponential factor [L mol^{-1} min^{-1}]
ΔH^o : enthalpy of the reaction [kJ mol^{-1}]
ΔS^o : entropy of the reaction [kJ mol^{-1} K^{-1}]
ΔG^o : free energy of the reaction [kJ mol^{-1}]
R : gas constant [kJ mol^{-1} K^{-1}]

REFERENCES

1. B. Erdem and M. Cebe, *Korean J. Chem. Eng.*, **23**, 896 (2006).
2. M. Sharma, R. K. Wanchoo and A. P. Toor, *Ind. Eng. Chem. Res.*, **53**, 2167 (2014).
3. S. H. Ali, *Int. J. Chem. Kinet.*, **41**, 432 (2009).
4. J. Lilja, J. Aumo, T. Salmi, D. Y. Murzin, P. Mäki-Arvela, M. Sundell, K. Ekman, R. Peltonen and H. Vainio, *Appl. Catal. A: Gen.*, **228**, 253 (2002).
5. L. Ma, Y. Han, K. Sun, J. Lu and J. Ding, *J. Energy Chem.*, **24**, 456 (2015).
6. T. A. Peters, N. E. Benes, A. Holmen, J. T. F. Keurentjes, *Appl. Catal. A: Gen.*, **297**, 182 (2006).
7. F. Leyva, A. Orjuela, D. J. Miller, I. Gil, J. Vargas and G. Rodríguez, *Ind. Eng. Chem. Res.*, **52**, 18153 (2013).
8. M. A. Tejero, E. Ramírez, C. Fité, J. Tejero and F. Cunill. *Appl. Catal. A: Gen.*, **517**, 56 (2016).
9. O. Ilgen, *Fuel Process. Technol.*, **124**, 134 (2014).
10. P. E. Jagadeeshbabu, K. Sandesh and M. B. Saidutta, *Ind. Eng. Chem. Res.*, **50**, 7155 (2011).
11. H. T. R. Teo and B. Saha, *J. Catal.*, **228**, 174 (2004).
12. A. Orjuela, A. J. Yanez, A. Santhanakrishnan, C. T. Lira and D. J. Miller, *Chem. Eng. J.*, **188**, 98 (2012).
13. Y. T. Tsai, H. M. Lin and M. J. Lee, *J. Taiwan Inst. Chem. Eng.*, **42**, 271 (2011).
14. B. Schmid, M. Döker and J. Gmehling, *Ind. Eng. Chem. Res.*, **47**, 698 (2008).
15. M. R. Altiokka and E. Ödeş, *Appl. Catal. A: Gen.*, **362**, 115 (2009).
16. M. T. Sanz, R. Murga, S. Beltrán, J. L. Cabezas and J. Coca, *Ind. Eng. Chem. Res.*, **41**, 512 (2002).
17. S. H. Ali, A. Tarakmah, S. Q. Merchant and T. Al-Sahhaf, *Chem. Eng. Sci.*, **62**, 3197 (2007).
18. W. Osorio-viana, M. Duque-bernal, J. Fontalvo, I. Dobrosz-gómez and M. Á. Gómez-garcía, *Chem. Eng. Sci.*, **101**, 755 (2013).
19. M. R. Altıokka and A. Çıtak, *Appl. Catal. A: Gen.*, **239**, 141 (2003).
20. A. Izci and F. Bodur, *React. Funct. Polym.*, **67** 1458 (2007).
21. A. H. M.Fauzi and N. A. S. Amin, *Energy Convers. Manage.*, **76**, 818 (2013).
22. M. C. De Jong, R. Feijt, E. Zondervan, T. A. Nijhuis and A. B. de Haan, *Appl. Catal. A: Gen.*, **365**, 141 (2009).
23. W. Mao, X. Wang, H. Wang, H. Chang, X. Zhang and J. Han, *Chem. Eng. Process.*, **47**, 761 (2008).
24. H. S. Fogler, *Elements of Chemical Reaction Engineering*, Prentice-Hall, Upper Saddle River, New Jersey, U.S.A. (1999).
25. G. D. Yadav and A. D. Murkute, *Int. J. Chem. React. Eng.*, **1**, 1 (2003).
26. P. Delgado, M. T. Sanz and S. Beltrán, *Chem. Eng. J.*, **126**, 111 (2007).
27. P. Yin, L. Chen, Z. Wang, R. Qu, X. Liu, Q. Xu and S. Ren, *Fuel*, **102**, 499 (2012).
28. C. H. Su, *Bioresour. Technol.*, **130**, 522 (2013).
29. Z. P. Xu and K. T. Chuang, *Can. J. Chem. Eng.*, **74**, 493 (1996).
30. A. K. Kolah, N. S. Asthana, D. T. Vu, C. T. Lira and D. J. Miller, *Ind. Eng. Chem. Res.*, **47**, 5313 (2008).